

Biosorption of Heavy Metals Using Plant-Derived Sorbents: An Environmental Solution for Industrial Wastewater

Anis Kumar M¹, Swarnalatha A P², Naveen K N³, Suryanarayana Raju J N S⁴, Shankramma S.Kerur⁵, Priyadharsini K^{6*}

¹Department of Biotechnology, V.S.B Engineering College, Karur, Tamilnadu 639111, India. (aniskumarmani@gmail.com)

²Department of Biomedical Engineering, V.S.B Engineering College, Karur, Tamilnadu 639111, India. (apglatha@gmail.com)

³Department of Electronics and Communication Engineering, Dayananda Sagar College of Engineering, Bengaluru, Karnataka 560078, India. (naveenkn-ece@dayanandasagar.edu)

⁴Department of Civil Engineering, S.R.K.R. Engineering College, Bhimavaram, Andhra Pradesh 534204, India. (jnssraju.srkrec@gmail.com)

⁵Department of Chemistry, KLE Technological University, Belagavi Campus, Dr. M.S. Sheshgiri College of Engineering & Technology, Karnataka 590008, India. (ksn2373@gmail.com)

^{6*}Department of Physics, Tagore Engineering College, Chennai, Tamilnadu 600127, India. (tecpriyaphy@gmail.com)

Abstract

This study used a biosorbent, derived from processed *Prosopis juliflora* root powder to treat wastewater and remove lead (Pb), cadmium (Cd), and copper (Cu) ions. The biosorption process was influenced by factors including temperature (25 to 65°C), biomass content (1 to 5 g), pH levels (1.0 to 7.0), and adsorbate concentration (10 to 50 mg/L). The absorption of lead and copper ions was investigated using batch sorption methods. The outcomes exhibited the maximum efficiency of adsorption achieved at a pH of 4.0, with the removal efficiencies of 94.92% for lead (Pb), 89.73% for cadmium (Cd), and 90.28% for copper (Cu). Even though the pseudo-first and second-order kinetics were considered, the experimental results aligned with the Freundlich isotherm model. Furthermore, the thermodynamic constants (ΔG° , ΔH° , and ΔS°) indicated that the Pb, Cd, and Cu metal ions adsorption using *Prosopis juliflora* root powder was feasible under the experimental conditions.

Keywords: Biosorption, Heavy metals, *Prosopis Juliflora*, Kinetic studies, Thermodynamic studies.

1 Introduction

Pollution is exacerbated by toxic compounds released into the environment by industrial activities such as smelting, mining, manufacturing, and use of metals in agricultural fertilizers and pesticides. In many developing nations with lax environmental regulations, untreated or

inadequately treated sewage is released into rivers, lakes, and seas (Tabrez et al., 2022). Due to ineffective wastewater management, heavy metal concentrations in water bodies and ecosystems increase. This accumulation of heavy metals poses serious risks to biodiversity and human health by introducing toxic substances into the food chain which leads to prolonged toxicity. The absence of stringent environmental regulations in numerous developing countries intensify the issue and renders them susceptible to significant ecological harm due to metal pollution (Uduakobong & Augustine, 2020). The buildup of heavy metals in aquatic environments disrupts ecosystems and threatens marine life. These contaminants ultimately infiltrate the food chain, affecting fish and other species consumed by humans. The ingestion of such contaminated organisms can lead to severe health repercussions including an elevated risk of cancer and various health conditions (Yogeshwaran & Priya, 2021). This challenge is not limited to specific regions; it impacts developed and developing nations. Immediate global intervention is essential to mitigate the consequences of heavy metal contamination in the environment and public health. Enhanced legislation, improved wastewater treatment processes, and increased public awareness are critical to address the sources and impacts of heavy metal pollution (Venkatraman & Priya 2021).

Human activities have increasingly contributed in releasing toxic heavy metals into the environment including cadmium, mercury, copper, and lead. Key sources of this pollution include mining operations, ore processing, the production of batteries and paints, and the extensive use of fossil fuels (Rupa et al., 2022). The insufficient enforcement of heavy metal emissions regulations pose significant risks to ecosystems and human health, underscoring the pressing need for improved regulatory frameworks and sustainable practices to alleviate these impacts. One of the critical strategies for safeguarding the environment and public health is the removal of heavy metals from wastewater. Biosorption emerges as an effective method for extracting hazardous contaminants from water by utilizing biomolecules that selectively bind to and sequester specific ions or molecules. This environmentally friendly water purification and waste treatment technique employ various biomasses, such as algae, fungi, bacteria, and plant leaves to eliminate heavy metals from contaminated water (Amit et al., 2022). Among the most harmful heavy metals, lead, cadmium, and copper pose serious risks to living organisms. Consequently, researchers are investigating alternative biomass sources for metal adsorption as a sustainable and eco-friendly approach to reduce heavy metal pollution and its associated environmental and health consequences (Chuanbin et al., 2022). This study used chemically treated *Prosopis juliflora* roots to develop an effective biosorbent. Although limited research has been conducted on the biosorption potential of plant roots, this investigation aims to assess the efficacy of *Prosopis juliflora* root biomass in removing heavy metals from contaminated environments and to compare its performance with other

biosorbents. *Prosopis juliflora* is an invasive, fast-growing tree native of South America but now widely distributed across arid and semi-arid regions of Africa, Asia, and the Middle East. Known for its hardiness and ability to thrive in harsh conditions, it is resistant to drought and can grow in nutrient-poor soils, making it useful for combating desertification. However, *Prosopis juliflora* is also problematic due to its aggressive spread which outcompetes the native vegetation and affects biodiversity (Yan et al., 2020). Despite its invasiveness, its wood is valuable for fuel, and its roots, bark, and pods have been explored for various applications including medicinal uses and as adsorbents for pollutants in environmental studies. In particular, its roots are being studied for their potential in adsorbing contaminants like heavy metals and dyes from water. The findings indicate that the *Prosopis juliflora* root biosorbent effectively adsorbs Pb, Cd, and Cu ions from simulated wastewater. Advanced technique like scanning electron microscopy (SEM), was employed to evaluate surface characteristics and conductivity and to identify the functional groups intricate in metal ion adsorption. The primary objective of this study is to investigate the potential of *Prosopis juliflora* root powder as an eco-friendly, low-cost adsorbent for removing heavy metal ions from aqueous solutions. This research aims to provide a sustainable and practical solution to the global challenge of heavy metal contamination in water, while promoting the utilization of an invasive plant species. The findings will not only contribute to the scientific understanding of biosorption but also have significant implications for environmental management and pollution control strategies.

2 Materials and Methods

2.1 Adsorbent preparation from the *Prosopis juliflora* roots

The roots of the *Prosopis juliflora* plant were harvested from Rameshwaram, situated in the southern region of Tamil Nadu, India. After thorough cleaning with distilled water, impurities and soluble contaminants were removed. The roots were air-dried at room temperature before being placed in a hot air oven at 333 K for 24 hours. The resulting dried biomass was ground into a fine powder using an electric grinder and cleaned thoroughly with distilled water. This biomass was dried in the oven at 333 K for two additional days. By following this drying process, the biomass was further reduced and filtered through a 63 μm mesh, resulting in particles, measuring 63 μm .

2.2 Metal ion solution

Analytical grade reagents were used in this study to prepare all the chemicals. The solutions and reagents were prepared using double distilled water. Stock solutions of the heavy metal standards were organized using analytical grade salts, Lead nitrate ($\text{Pb}(\text{NO}_3)_2$), cadmium nitrate ($\text{Cd}(\text{NO}_3)_2$), and copper sulphate pentahydrate ($\text{CuSO}_4 \cdot 5\text{H}_2\text{O}$) in distilled water to which 3.0 cm^3 concentrated HNO_3 acid had been added, and then diluted to 1.0 Litre. The working standard metal solutions were obtained by diluting appropriate amounts of heavy metal solution using distilled

water. A few drops of Caesium-lanthanum (CsCl/LaCl₃; 5:20 g/L) solution were added to each working standard as an interference suppressant. The initial pH of the solutions during the analyses was adjusted using 0.1 M HCl or 0.1 M NaOH.

2.3 Batch Adsorption Experiment

The experiments were done in 100 mL polypropylene bottles at 20°C using a rotary shaker at 65rpm. Optimized experimental conditions include particle size, contact time, pH, initial metal ion concentration, and temperature. This was done by keeping all other parameters constant while varying the one parameter under consideration. 0.1g of adsorbent was placed in a polypropylene bottle, followed by 100mL of the desired metal ion concentration, and then placed in the shaker for 60 minutes. The effects of optimizing parameters were studied, and each shaken solution was filtered through the Whatman filter paper. Then, the metal ion concentration of the filtrate was determined. All determinations were triplicated using a flame atomic absorption spectrophotometer (AAS). Equations 1 and 2 can be used to determine the adsorption process's efficiency.

$$\text{Removal efficiency (\%)} = \frac{(C_i - C_o)}{C_i} \times 100 \quad (1)$$

$$Q_e = \frac{(C_o - C_i) \cdot V}{m} \quad (2)$$

2.4 Evaluation of the PJRP Properties

The biosorbent's morphology was assessed using Scanning Electron Microscopy (SEM) before and after chemical activation. This enabled the visualization of surface alterations such as increased porosity and texture modifications resulting from the activation process. FTIR spectrometry was used to classify and compare the efficient groups in the biosorbent before and after its interaction with metal ions. This analysis is crucial for understanding the binding sites and chemical interactions between the biosorbent and the metal ions (Candamano et al., 2022). Additionally, thermal decomposition atomic absorption spectrometry was employed to analyze all samples to detect and quantify metal ions. The instrument featured an exceptionally low detection limit of 0.001 ng, ensuring accurate detection of trace metal concentrations. To ensure the reliability of the mercury analysis, the instrument's accuracy was validated by examining a certified reference material from sediment.

2.5 pH – Zero Point Change

The determination of the biosorbent's zero-point charge (pHzpc) was conducted utilizing the solid addition method. This approach elucidates the pH level at which the surface of the biosorbent achieves electrical neutrality. The experiment is instrumental in comprehending the adsorption characteristics of the biosorbent across varying pH conditions (Ahmed et al., 2022). The

methodology involved using 0.1 M potassium nitrate (KNO_3) as the electrolyte. A 50 ml aliquot of potassium nitrate solution was poured in a 250 ml conical flask, and the initial pH was meticulously adjusted to a range between 2.0 and 10.0. Around 0.1 gm of PJRP was added to the metal ion solution. The solution was shaken for 24 hours at 150 rpm using the rotary shaker to ensure the interface between the adsorbate and metal ions. The metal ion solution's final pH (pH_f) was verified after 24 hours. The final and initial pH variations were calculated using the relationship of $\Delta\text{pH} = \text{pH}_o - \text{pH}_f$. A graph was subsequently generated with the initial pH (pH_o) plotted on the x-axis and ΔpH on the y-axis. The pH_{zpc} of the PJRP biosorbent was identified at the point where the curve intersects the x-axis, signifying the pH at which the biosorbent surface exhibited a net neutral charge.

2.6 Desorption studies

Following the biosorption of metal ions under batch conditions, we conducted desorption experiments utilizing sulfuric acid (H_2SO_4) as an eluting agent. This methodology was employed to evaluate the reusability of both natively and chemically modified PJRP biosorbents across successive biosorption-desorption cycles. For the desorption experiment, the biosorbent loaded with metal ions from the prior biosorption phase was oven-dried and placed in a 250 ml conical flask holding 50 ml of the H_2SO_4 desorbing solution. The experimental parameters, including contact time and agitation speed, were consistent with those applied during the biosorption phase. Upon the completion of the desorption process, the regenerated biosorbent was carefully washed with distilled water to eliminate the residual H_2SO_4 . The cleaned biosorbent was then dried in a hot air oven, prepared it for subsequent biosorption cycles. This procedure was repeated up to three consecutive biosorption-desorption cycles to evaluate the biosorbent's reusability and capacity to retain efficiency over multiple cycles. Such an assessment is crucial for determining the long-term viability of PJRP as a sustainable biosorbent.

3 Results and Discussion

3.1 Adsorbent characterization

FTIR spectra were obtained for both the untreated biomass and the biomass loaded with metal ions, covering a spectral range of 400–4000 cm^{-1} . This investigation aimed to identify the specific functional groups that engage with metal ions during the biosorption process. Figure 1 illustrates the peaks of the chemically activated *Prosopis juliflora* root powder which are loaded with metal ions (Pb, Cu, and Cd) in the respective order. The broad bands observed in Figure 1, from 3526.11 to 3749.66 cm^{-1} , suggest the presence of amine ($-\text{NH}$) or hydroxyl ($-\text{OH}$) groups. The carbonyl ($-\text{C}-\text{O}$) stretching group attribution was observed at the peak of 1717.76 cm^{-1} . The FTIR spectra reveal distinctive functional groups within the *Prosopis juliflora* root powder biomass.

The carbon atoms (-CH) and aldehyde (-CHO) groups were associated with the peaks at 2884.76 cm^{-1} and 2945.96 cm^{-1} , respectively. Furthermore, the C-O stretching was discovered at a notable peak range of 1320–1000 cm^{-1} , typically linked to alcohols and carboxylic acids (Priya et al., 2022). A critical observation from the FTIR spectra in peak positions following the adsorption of metal ions. Specifically, the peaks at 3526.11, 3749.11, and 1771.76 cm^{-1} were found shifting to 3504.35, 3743.31, and 1773.71 cm^{-1} , demonstrating the interaction and uptake of metal ions by the -OH and C-O functional groups. The C-O stretching vibrations associated with alcohols and carboxylic acids were initially observed at 1314.74 cm^{-1} and shifted to 1365.79 cm^{-1} post-biosorption (Jayachandran et al., 2021). SEM images were captured before and throughout the biosorption process.

In Figure 2(a), the SEM image illustrates the biosorbent's porous architecture before biosorption, while Figure 2(b) depicts the biosorbent post-biosorption, revealing the incorporation of Pb, Cd, and Cu ions. These SEM images provide intricate three-dimensional surface representations, facilitating a comprehensive assessment of the structural modifications during biosorption. Notably, Figure 2(b) reveals a filamentous structure interspersed with porous features, likely resulting from the heterogeneous surface composition of the powder (Mohammed et al., 2021). Analyzing surface attributes are essential for recognizing potential binding sites for the targeted pollutants, akin to the mechanisms observed in physical biosorption. Based on the characterization process, it was confirmed that the adsorbent can remove contaminants from the water.

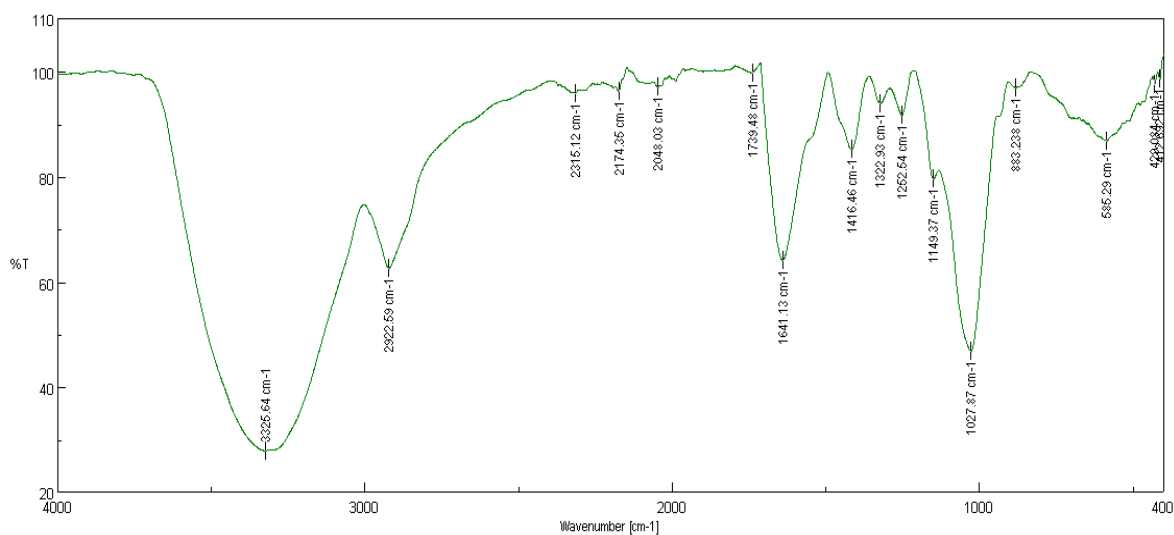
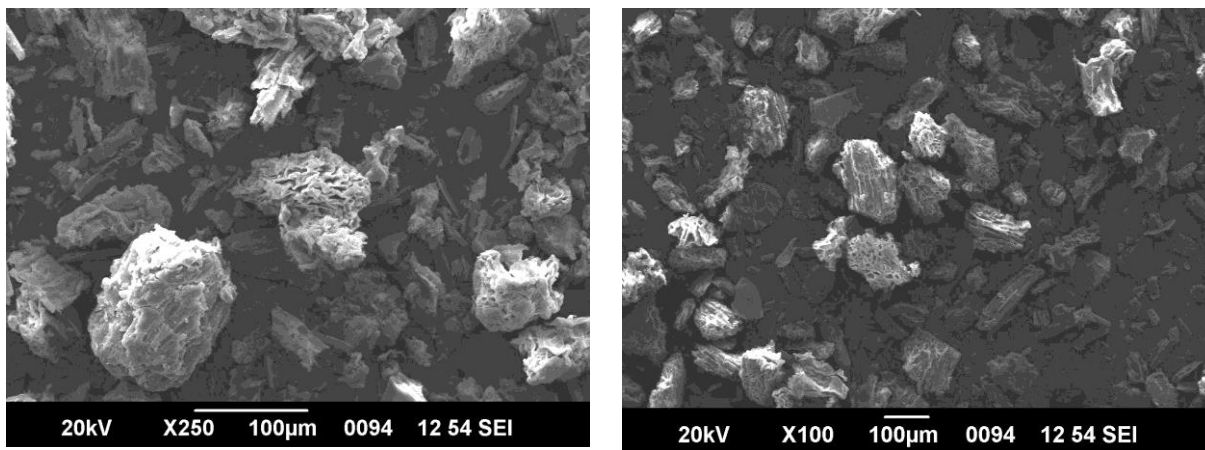


Figure 1 FTIR peaks of Raw PJRP adsorbent



(a)

(b)

Figure 2 (a) Raw and (b) metal ions adsorbed PJRP biosorbent SEM image

3.2 Impact of pH in metal ion adsorption

To improve the effectiveness of the adsorption process, it is important to optimize the pH level. Understanding the relationship between the ionization of functional groups, the adsorbate speciation and the biosorbent's surface charge are crucial for efficient contaminant removal. The negatively charged ions on the surface of *Prosopis juliflora* root powder play a significant role in the biosorption process (Ramiro et al., 2022). This research investigated the effects of pH values ranging from 1.0 to 7.0 on the adsorption capacities of Pb, Cd, and Cu ions. Figure 3 depicts the biosorption performance of PJRP across various pH levels. The results showed that, increasing the pH from 1.0 to 4.0 improved the elimination of Pb, Cd, and Cu ions, but the removal efficiency decreased afterwards. At lower pH levels (1.0 to 3.0), the competition between negatively charged H_3O^+ ions and positively charged metal ions improved biosorption efficiency. However, at pH 4.0, the biosorption effectiveness diminished as Pb, Cd, and Cu ions interacted with hydroxide ions. The study identified peak removal efficiencies at pH 4.0, with Pb achieving 90.2%, Cu 94.9%, and Cd 88.5%.

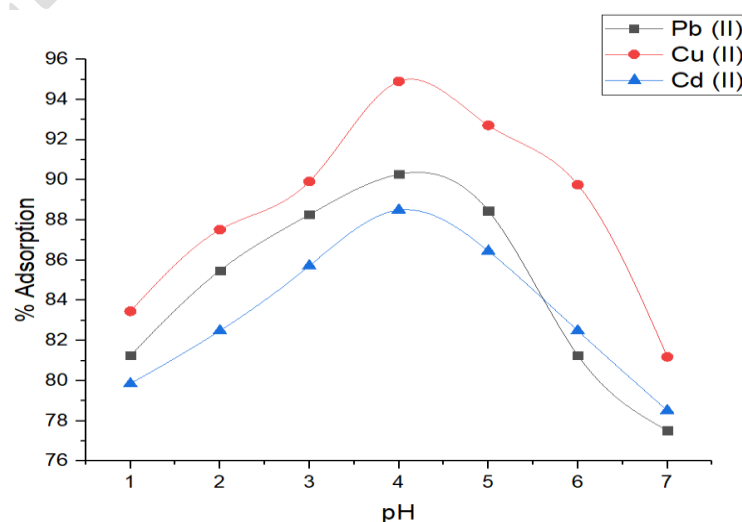


Figure 3 Effect of pH variation on adsorption efficiency

3.3 Impact of biochar dose

This study investigates the influence of varying quantities of biosorbent on the extraction of metal ions. Specifically, we incorporated 1 to 5 grams of biochar into synthetic solutions which contain ten mg/L concentrations of Pb, Cd, and Cu ions. By following the prior research to establish the optimal pH, we adjusted the solution's pH accordingly. The mixture was agitated for 45 minutes at 25°C and 170 rpm. As illustrated in Figure 4, the quantity of biosorbent significantly impacts the efficacy of removal of metal ions using *Prosopis juliflora* root powder (PJRP). Notably, an increased biosorbent amount up to 3.0 grams enhanced removal efficiency. Adding more biosorbents increases the number of available biosorption sites without leading to saturation (Serdar et al., 2021). The optimal dosage of 3.0 grams achieved maximum biosorption efficiencies of 95.63% for Cu^{2+} , 90.27% for Cd^{2+} , and 89.71% for Pb^{2+} . However, further increases in biosorbent concentration did not yield additional improvements in removal efficiency likely due to the aggregation of the biosorbent, the accessible surface area for adsorption was diminished.

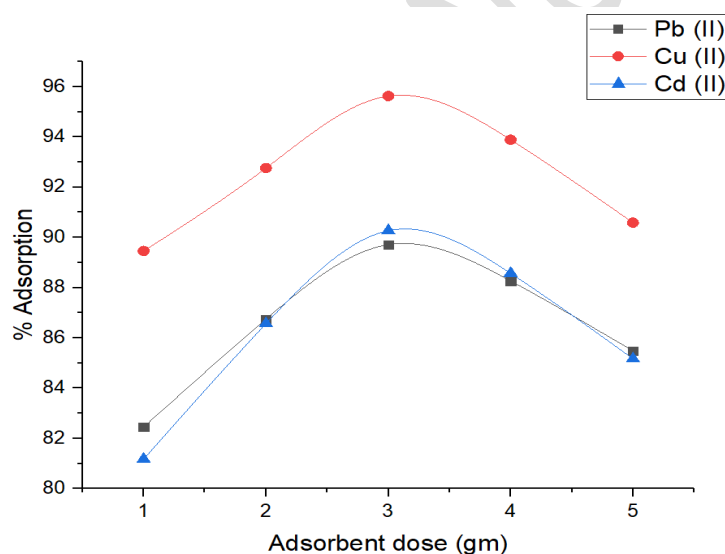


Figure 4 Effect of adsorbent dose variation on adsorption efficiency

3.4 Impact of ion concentration

The concentrations were varied from 10 to 50 ppm, maintaining a pH of 4.0, using 3.0 grams of biosorbent and allowing for 45-minutes interaction at room temperature. Figure 5 demonstrates the removal rates for Pb^{2+} ions fell from 93.63% to 65.47%, for Cu^{2+} ions from 89.27% to 69.5%, and for Cd^{2+} ions from 82.39% to 70.28% as the initial concentrations increased. The highest concentration of metal ions saturates the accessibility of adsorbent sites in the PJRP and gradually decreases efficiency. The reduction in the rate of metal ion adsorption with a rise in the initial concentration occurs due to the saturation of adsorbent sites (Hana et al., 2021). Additionally,

Figure 5 shows that higher initial metal ion concentrations result in a greater amount of metal adsorbed per unit mass of biosorbent due to the larger concentration gradient that enhances the transfer of metal ions from the liquid phase to the solid phase.

3.5 Impact of Reaction Time

This research examined contact times that spanned from 10 minutes to 1 hour. As illustrated in Figure 6, the removal of metal ions commenced rapidly but exhibited a significant decline after 50 minutes. At this juncture, the removal rates for all metal ions stabilized, showing no further substantial increases in ion capture. This stabilization was attributed to the saturation of the biosorbent surface, which resulted in repulsive forces that impeded additional absorption of metal ions (Melania et al., 2021). Furthermore, with prolonged contact times, mass transfer efficiency from the liquid phase to the solid phase was diminished. The heavy metal ions were required to traverse through densely packed pores over extended distances, decreasing the overall adsorption efficiency.

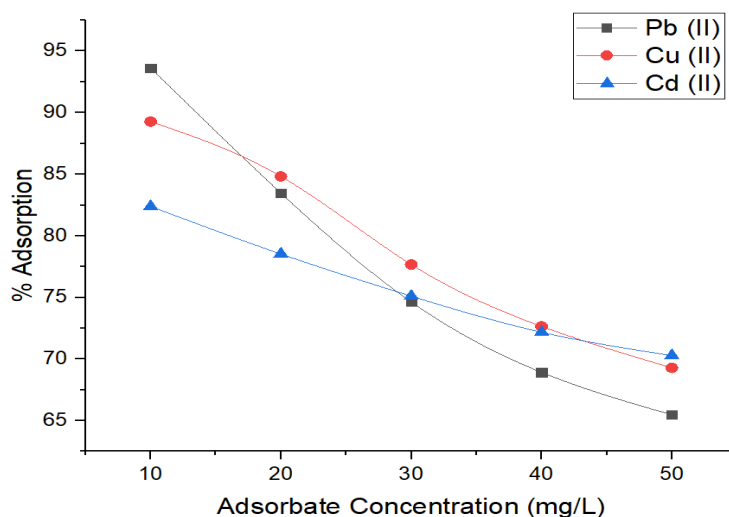
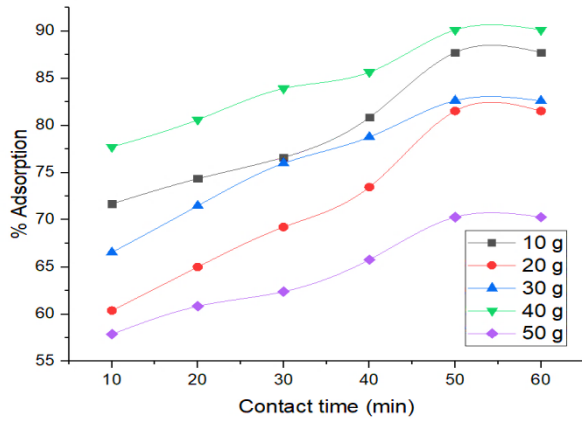


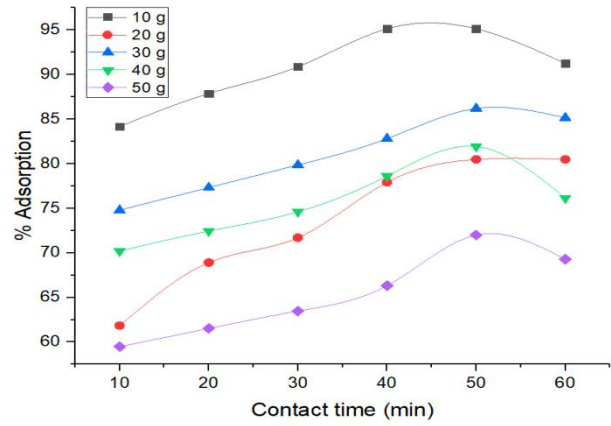
Figure 5 Effect of adsorbate concentration variation on adsorption efficiency

3.6 pH – Zero-point change

The pH_{zpc} value of 4.96 for the PJRP biosorbent is significant in understanding its adsorption characteristics (Figure 7). In alkaline pH conditions it exceeds the pH_{zpc} value, the biosorbent's surface charge turns negative, thereby enhancing its capacity to adsorb cations such as Pb(II), Cu(II), and Cd(II). This observation is consistent with your results, indicating that adsorption efficiency is heightened under these circumstances. In contrast, when the pH falls below the pH_{zpc} , the surface charge shifts to positive, promoting the adsorption of anions (Nyemaga et al., 2021). This knowledge elucidates the biosorbent's efficacy across different pH levels, particularly its superior performance in alkaline environments.



(a)



(b)

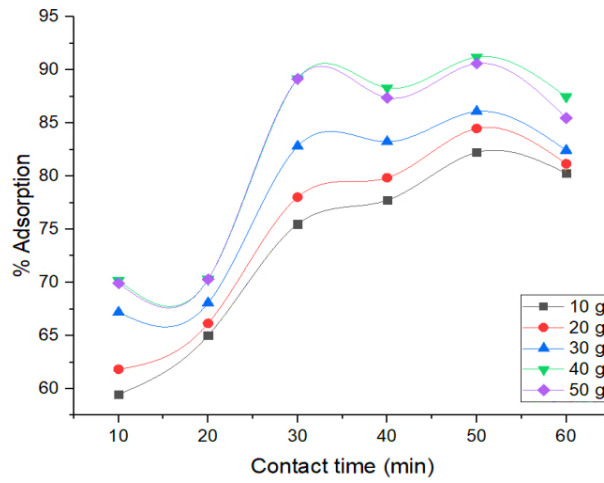


Figure 6 Effect of reaction time variation on adsorption efficiency for (a) Pb, (b) Cd, and (c) Cu ions

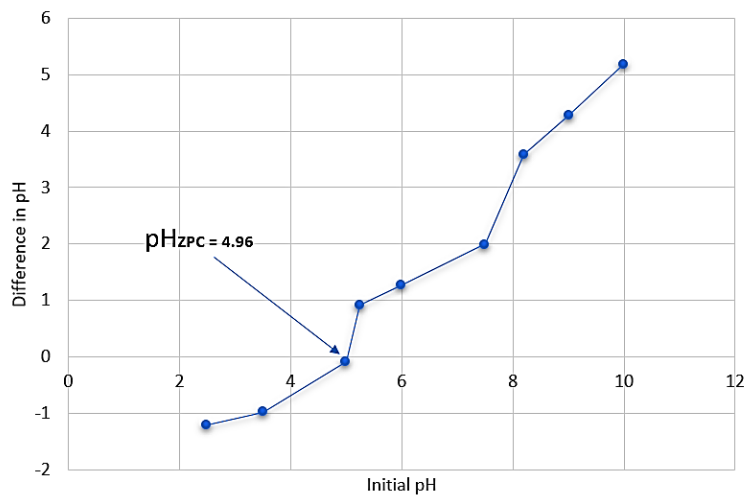


Figure 7 pH_{ZPC} of the batch adsorption studies

3.7 Isotherm studies

3.7.1 Langmuir study

The Langmuir isotherm model posits that biosorption occurs as a monolayer on a consistent and uniform biosorbent surface. It is based on the premise that a limited number of specific biosorption sites exist with each site capable of adsorbing only a single molecule or ion (Nadir et al., 2020). Equation 3 represents the linear form of this isotherm model.

$$q_e = \frac{q_{max}R_L C_e}{1 + R_L C_e} \quad (3)$$

The model derives the values of q_{max} and R_L from the direct association between C_e/q_e and C_e , as depicted in Figure 8. This figure demonstrates the relationship between the concentrations of metal ions in the solution and the corresponding amounts of these ions adsorbed per unit mass (g) of *Prosopis juliflora* root powder (PJRP). The R^2 values are 0.9704 for Pb, 0.9673 for Cu, and 0.9505 for Cd, indicating a strong fit of this isotherm model to the equilibrium data and its utility in forecasting the adsorption process. The R_L value can signify four distinct scenarios: linear ($R_L = 1$), irreversible ($R_L = 0$), positive ($0 < R_L < 1$), and negative ($R_L > 1$). Table 1 illustrates that the R_L values for Pb, Cd, and Cu ions range between 0 and 1, affirming the adsorption method's efficacy.

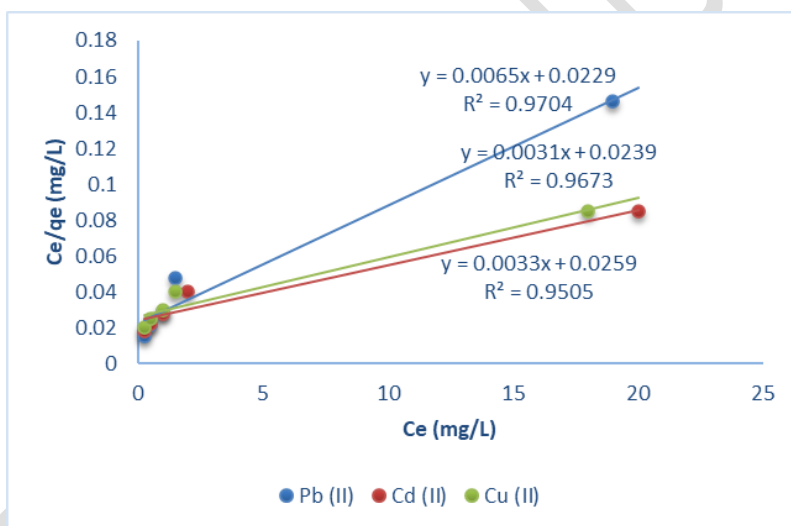


Figure 8 Langmuir isotherm plot for heavy metal adsorption using *Prosopis juliflora* roots

3.7.2 Freundlich isotherm

It is an empirical equation that provides insight into biosorption on heterogeneous surfaces. It suggests that adsorption occurs at sites with different energy levels, leading to the possibility of multilayer biosorption. This model considers the variations in adsorption capacity across different surface sites, unlike the Langmuir model, which operates under the assumption of uniform adsorption sites (Jayachandran et al., 2021). The equation for the Freundlich isotherm is expressed as follows.

$$q_e = K_f C_e^{\frac{1}{n}} \quad (4)$$

By plotting the $\log q_e$ vs $\log C_e$, one can derive the parameters K_f and $1/n$ pertinent to the Freundlich isotherm model. Table 1 presents the correlation coefficients and isotherm constants

associated with this model. A comparison with the Langmuir model reveals that the Freundlich model yields lower correlation coefficients, suggesting that the Langmuir model offers a greater fit for the adsorption data. Within the Langmuir framework, the q_{\max} value signifies the maximum monolayer saturation at equilibrium, which suggests the biosorbent's adsorption capacity. The K_f and $1/n$ values in the Freundlich model reflect varying affinities for metal ions. The regression coefficients for Pb, Cd, and Cu ions are recorded as 0.9891, 0.9557, and 0.9656, respectively. A higher $1/n$ value suggests an increased affinity and a wider array of adsorption sites in the biosorbent preparation.

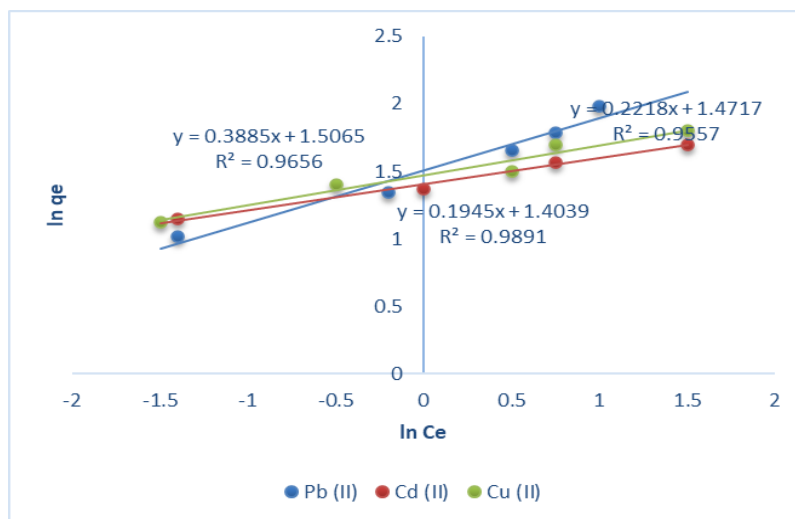


Figure 9 Freundlich isotherm plot for heavy metal adsorption using Prosopis juliflora roots

3.7.3 Sips isotherm study

The Sips isotherm is a composite model that amalgamates characteristics from the Langmuir and Freundlich isotherms. It is frequently used to characterize biosorption on heterogeneous surfaces, akin to the Freundlich model, while incorporating the Langmuir idea of monolayer adsorption. By introducing a saturation limit, the Sips isotherm addresses the shortcomings of the Freundlich model at elevated adsorbate concentrations, a consideration that the Freundlich equation does not include (Adewumi et al., 2021). The equation representing the Sips isotherm is given as:

$$q_e = \frac{q_{\max} K_s C_e^n}{1 + K_s C_e^n} \quad (5)$$

In this equation, q_e represents the adsorbed amount of metal ions per unit mass during the equilibrium (mg/g), the capacity of adsorption is represented by q_{\max} (mg/g), and C_e represents the concentration in equilibrium (mg/L). The Sips isotherm constant, denoted as K_s , indicates the attraction of the PJRP onto the metal ions. At the same time, n is a dimensionless factor reflecting the system's heterogeneity. The constants Q_{\max} and K_s for the Sips model were determined from the slope and intercept values illustrated in Figure 10. These constants and the regression criteria are presented in Table 1. An R^2 value greater than 0.95 confirms that the Sips model accurately

describes the metal ion adsorption data. This process is influenced by the variable n , which ranges from 0 to 1. When n approaches 1, the Sips model aligns more closely with the Langmuir model, indicating a more uniform adsorption behaviour.

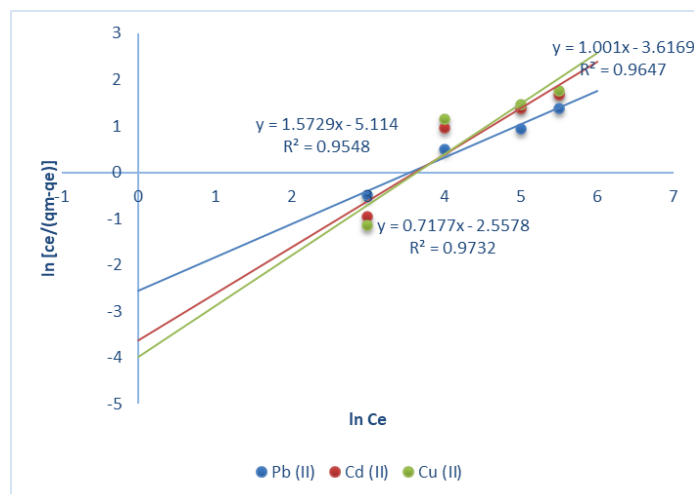


Figure 10 Sips isotherm plot for heavy metal adsorption using Prosopis juliflora roots

Table 1 Constants of isotherm studies for the adsorption of metal ions using PJRP

Isotherm Model	Types of metal ions			
	Parameters	Pb II	Cd (II)	Cu (II)
Langmuir	q_{\max} (mg/g)	9.037	9.128	8.923
	R_L (L/mg)	0.228	0.261	0.205
	R^2	0.9704	0.9505	0.9673
Freundlich	K_f ((mg/g) (L/mg) ^{1/n})	2.729	1.951	1.657
	n (g/L)	2.854	2.253	1.928
	R^2	0.9656	0.9557	0.9891
Sips	K_S (bar ⁻¹)	13.246	7.542	3.057
	β_S (mmol g ⁻¹)	1.324	1.682	1.619
	as	0.512	0.346	0.252
	R^2	0.9548	0.9647	0.9732

3.8 Kinetic studies

3.8.1 Pseudo – First Order

In the biosorption process, this kinetic model is commonly applied to describe the kinetics during the early stages of the process. Equation 6 represents the linear form of this model.

$$\log(q_e - q_t) = \log q_e - \frac{k_1 t}{2.303} \quad (6)$$

Figure 11 illustrates the progression of $\log(q_e - q_t)$ over time which is instrumental in determining the values of k_1 and Q_e . The characteristics of these parameters can be established by

evaluating the slope and intercept of the linear relationship. Table 2 provides the R^2 correlation coefficient, which serves as an indicator of the model's fit. The study's results indicated no significant correlation between solute release and metal ion adsorption by the charcoal adsorbent, as demonstrated in the linear graphs. This finding suggests that the uptake of metal ions by PJRP is not solely due to physical adsorption mechanisms.

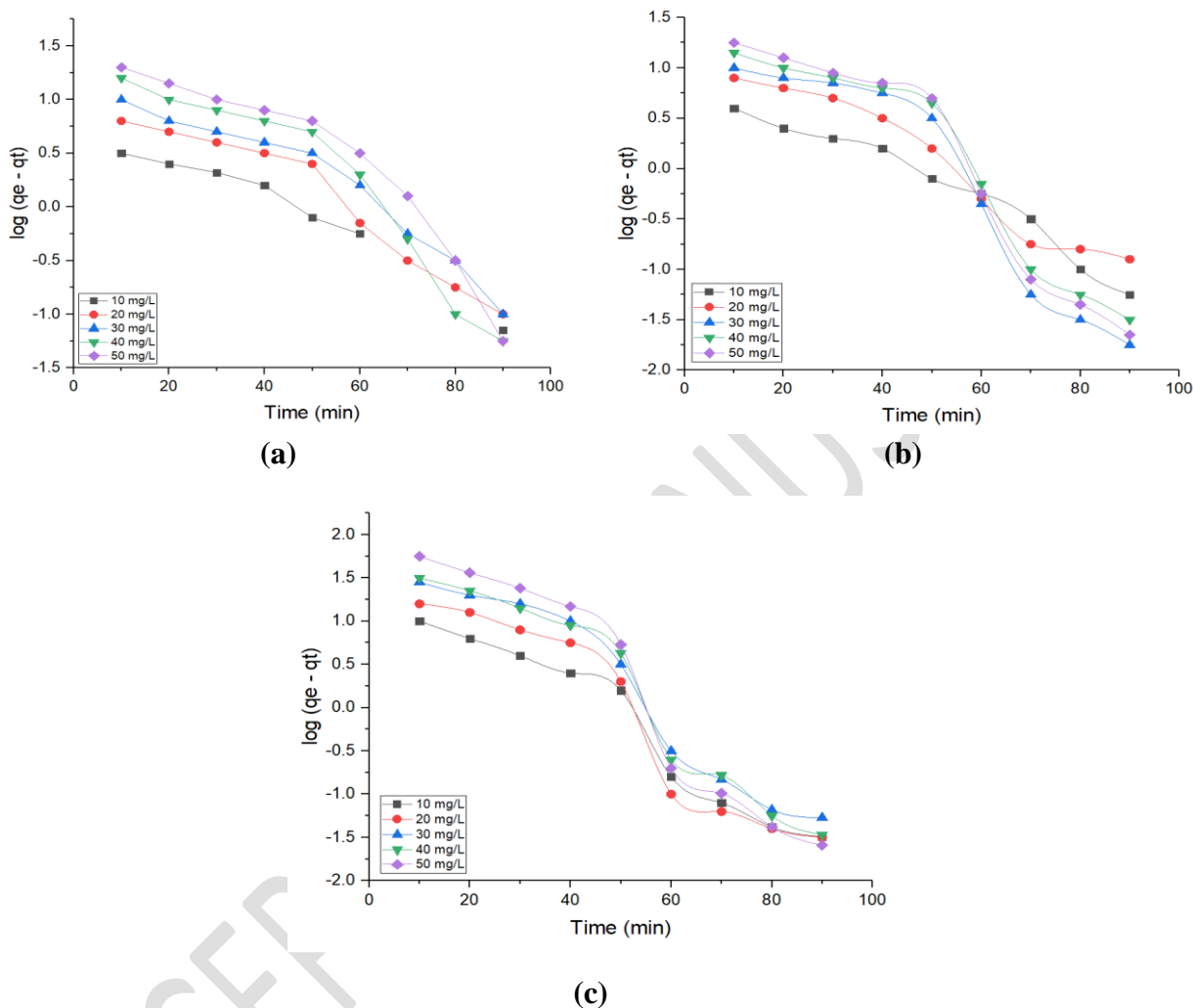


Figure 11 Pseudo-first-order kinetic plots for (a) Pb, (b) Cd, and (c) Cu metal ion adsorption

3.8.2 Pseudo-Second Order

This kinetic model serves as a prevalent framework for describing the biosorption process particularly in instances where the rate-limiting step is associated with the adsorption process of a chemical nature. The biosorbent surface area and the adsorbate concentration depend on the biosorption rate (Jinzhen et al., 2022). The linear equation of this kinetic equation is represented as:

$$\frac{t}{q_t} = \frac{1}{k_2 q_e^2} + \frac{t}{q_e} \quad (7)$$

The parameter k_2 represents the rate constant associated with this model, measured in g/mg min . In Figure 12, the determination of k_2 is achieved by analyzing the association between the ratio

of t/q and t . Table 2 provides the correlation coefficients for Pb, Cd, and Cu ions, alongside the kinetic parameters derived from Figures 11 and 12 for two distinct kinetic models. These parameters are essential for elucidating the biosorbent's effectiveness in adsorbing and removing heavy metals. The pseudo-first-order kinetic coefficients for Pb, Cd, and Cu are recorded as 0.9811, 0.9657, and 0.9787, respectively. In contrast, this kinetic model demonstrates high R^2 values of 0.9961, 0.9973, and 0.9952 for Pb, Cd, and Cu ions, respectively. The experimental findings highlight the biosorption capacity of the monolayer. Fluctuations in the adsorption of heavy metals during the biosorption process are likely attributable to the varying affinities of the metal ions for the active sites on the biosorbent material.

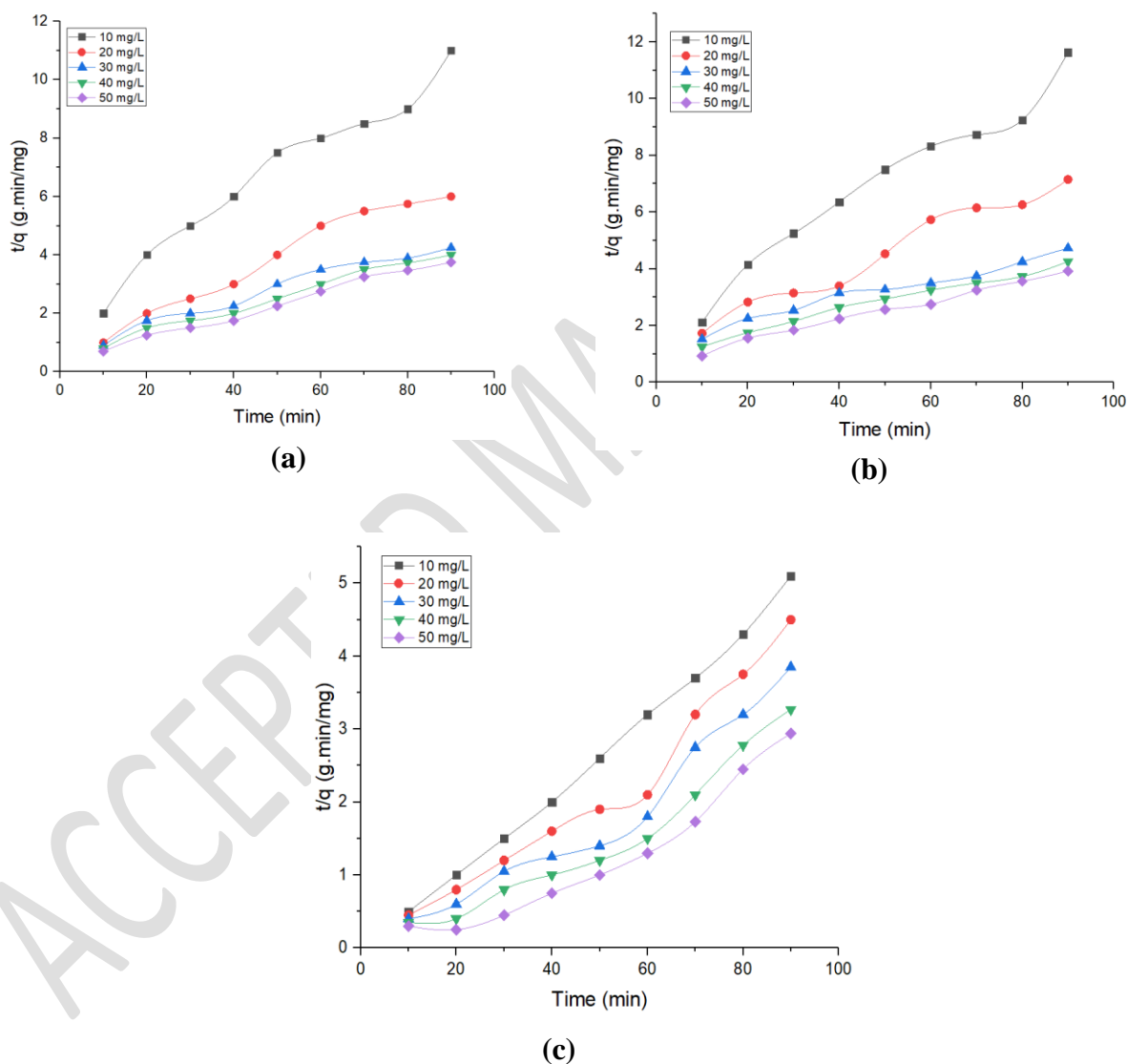


Figure 12 Pseudo-second-order kinetic plots for (a) Pb, (b) Cd, and (c) Cu metal ion adsorption

3.8.3 Boyd kinetic study

The Boyd kinetic model is applied to ascertain the rate-controlling step in the biosorption process, specifically distinguishing between film diffusion and intraparticle diffusion. This model is

essential for understanding whether adsorption kinetics are regulated by diffusion through the external boundary layer or by the diffusion occurring within the pores of the adsorbent particles. Equation 8 represents the linear form of this kinetic model.

$$B_t = -0.4977 - \ln(1 - F) \quad (8)$$

The Boyd function, denoted as B_t at time 't,' is utilized with the fractional adsorption F , which can be calculated using the formula $F = q_t/q_e$. This model is instrumental in determining the dominant diffusion mechanism within the biosorption process. The "Bt versus t" graph is critical for analyzing the linearity of the experimental results. The slowest step of the adsorption process due to intra-particle diffusion confirms the linear relationship produced from the origin (Long et al., 2021). Conversely, the adsorption of metal ions by PJRP influenced by external or film diffusion confirms the linear plots do not intersect the origin. Figures 12 (a), (b), and (c) present the plots corresponding to different concentrations of Pb, Cd, and Cu on PRJP. The calculated values of D_i and B from these plots are detailed in Table 1, along with the regression coefficient R^2 .

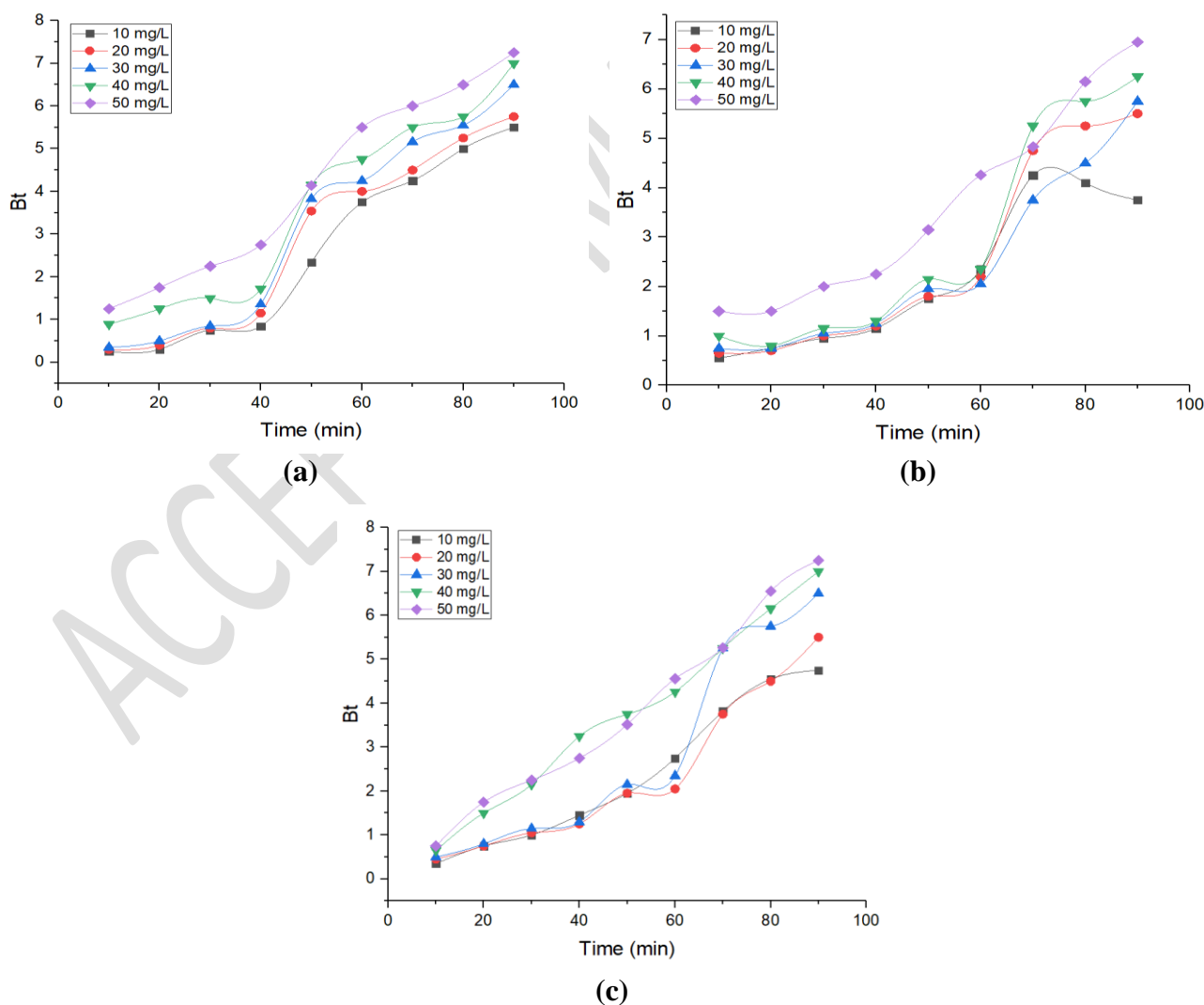


Figure 12 Boyd kinetic plots for (a) Pb, (b) Cd, and (c) Cu metal ion adsorption

Table 2 – Kinetic constants of metal ion adsorption process using Prosopis juliflora roots

S. No.	Nature of the metal ion	Concentration of the ion solution (mg/L)	Pseudo First Order			Pseudo Second Order					Boyd		
			k (min ⁻¹)	q _e , cal (mg/g)	R ²	K (g/mg.min) x 10 ⁻³	q _e , cal (mg/g)	h (mg/g.min)	q _e , exp (mg/g)	R ²	B	D _i (x 10 ⁻³ m ² /s)	R ²
1.	Pb II	10	0.0668	11.492	0.918	8.980	13.988	1.751	12.983	0.997	0.086	11.942	0.918
2.		20	0.0736	28.504	0.921	4.722	26.878	3.607	25.126	0.997	0.074	12.605	0.912
3.		30	0.0760	46.559	0.927	2.826	41.766	3.986	38.214	0.996	0.076	12.848	0.928
4.		40	0.0829	83.716	0.946	1.969	56.552	4.552	50.873	0.995	0.083	14.207	0.944
5.		50	0.0714	84.139	0.936	1.353	66.763	4.793	59.129	0.994	0.085	14.762	0.938
1.	Cd II	10	0.0678	12.445	0.927	7.763	13.968	1.522	12.840	0.997	0.068	11.492	0.928
2.		20	0.0714	29.040	0.911	3.600	26.513	2.778	24.450	0.997	0.072	12.373	0.914
3.		30	0.0737	54.935	0.928	2.870	38.642	3.623	36.892	0.979	0.086	14.354	0.925
4.		40	0.0875	84.121	0.924	1.530	51.235	4.617	48.711	0.969	0.088	14.730	0.927
5.		50	0.0921	94.189	0.931	0.949	62.458	4.655	59.122	0.994	0.093	15.177	0.931
1.	Cu II	10	0.0645	11.561	0.916	8.186	13.514	1.495	12.631	0.975	0.066	10.895	0.912
2.		20	0.0737	30.794	0.922	4.250	25.641	2.466	24.221	0.976	0.072	12.605	0.922
3.		30	0.0898	69.343	0.935	2.522	37.307	3.640	35.015	0.964	0.090	15.120	0.936
4.		40	0.0806	74.989	0.930	1.478	52.363	4.908	47,234	0.965	0.083	14.782	0.930
5.		50	0.0875	92.336	0.935	1.258	66.672	5.392	59.286	0.972	0.088	13.520	0.935

3.9 Thermodynamic studies

The rise in adsorption, as temperature rises, it indicates an endothermic process that may be thermodynamically described by calculating quantities like change in free energy (ΔG°), enthalpy (ΔH°), and entropy (ΔS°). The following equations 9 and 10 were used to determine these parameters:

$$\Delta G^\circ = -RT \ln K_L \quad (9)$$

$$\ln K_L = -\frac{\Delta G^\circ}{RT} = -\frac{\Delta H^\circ}{RT} + \frac{\Delta S^\circ}{RT} \quad (10)$$

K_L and Q_{ob} , the adsorption process's equilibrium constants (L/mg), are the same. The temperature in absolute terms is denoted by T, and the gas constant by R. The thermodynamic constants for the adsorption of metal ions are depicted in Figure 13. Table 3 provides a comprehensive summary of the thermodynamic constants, which include the variations in ΔS° , ΔH° , and ΔG° . The study employed and established the methodologies to derive these values. Results indicate that free energy consistently decreases as temperature increases, suggesting that metal ion adsorption is spontaneous and more advantageous at higher temperatures (Prasanna et al., 2021). The positive enthalpy changes signify that the biosorption process is endothermic with heat absorption contributing to enhanced reaction efficiency. Additionally, the positive entropy change reflects an increase in chance at the solid-liquid edge, indicating the effectiveness of the biosorption process under the studied conditions.

Table 3 Thermodynamic constants of the metal ion adsorption using PJRP

Pb II concentration	ΔH° (KJ/mol)	ΔS° (J/mol/	ΔG° (kJ/mol)			
			15°C	30°C	45°C	60°C
10	-32.764	-80.723	-8.299	-7.587	-7.116	-6.942
20	-20.134	-42.542	-6.396	-6.244	-6.102	-5.632
30	-18.678	-36.923	-5.809	-5.568	-5.314	-4.449
40	-13.452	-25.766	-5.079	-4.888	-4.637	-4.135
50	-11.823	-21.145	-4.233	-4.214	-3.924	-3.752
Cd II concentration						
10	-19.277	-45.892	-6.810	-5.563	-5.238	-4.381
20	-13.723	-27.922	-4.892	-4.528	-4.347	-4.082
30	-10.984	-21.114	-3.962	-3.153	-3.196	-3.080
40	-9.823	-22.276	-2.183	-2.160	-2.377	-2.119
50	-7.546	-20.091	-1.182	-1.363	-1.246	-1.204

Cu II concentration						
10	-13.376	-28.491	-5.807	-4.671	-4.398	-4.162
20	-11.036	-23.881	-4.099	-3.484	-3.425	-3.298
30	-9.311	-20.392	-3.154	-2.920	-2.771	-2.458
40	-8.741	-21.923	-2.283	-2.056	-1.845	-1.648
50	-7.293	-18.467	-1.957	-1.414	-1.265	-1.029

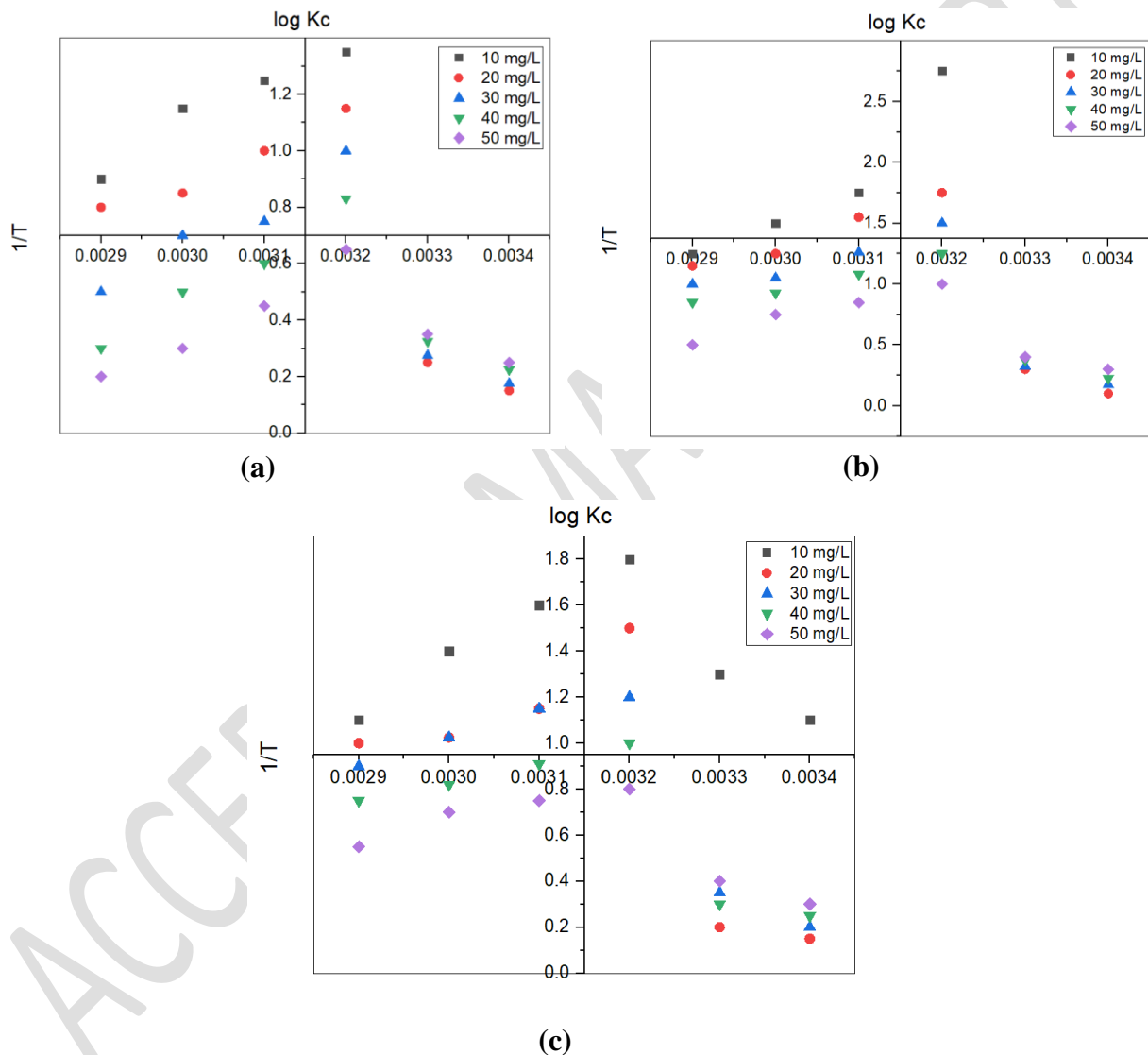


Figure 13 Thermodynamic plots for (a) Pb, (b) Cu, and (c) Cd metal ions using PJRP

3.10 Batch desorption study

The efficiency of removing metal ions from spent adsorbent (PJRP) depends greatly on how well the desorption process works. According to Table 4, desorption studies using different sulfuric acid concentrations (ranging from 0.1 to 0.4 N) showed that higher concentrations of sulfuric acid

led to better recovery of heavy metal ions, reaching its peak at 0.3 N H₂SO₄. However, beyond this concentration, there was no significant improvement in recovery. Therefore, the best solution for desorbing metal ions from spent PJRP was found to be 0.3 N H₂SO₄. Furthermore, the PJRP was regenerated and used again as an adsorbent in future tests.

Table 4 Desorption studies of metal ions using sulfuric acid

Initial concentration (10 mg/L)	Efficiency of metal ion removal (%)	Concentration of H ₂ SO ₄			
		0.10 N	0.20 N	0.30 N	0.40 N
		% Desorption of metal ions			
Pb II	94.92	79.28	82.67	88.59	84.73
Cd II	89.73	67.51	72.29	79.67	73.82
Cu II	90.28	69.59	75.54	80.59	76.13

Table 5 provides the comparative study of adsorption of metals ions with PJRP and other adsorbents. The efficiency and cost-effectiveness of *Prosopis juliflora* root powder as a biosorbent can be assessed by comparing it with other commonly used biosorbents, such as agricultural waste, algae, and other plant-based materials. *Prosopis juliflora* root powder stands out as an efficient and cost-effective biosorbent, particularly for areas where it is invasive. While algae may have higher adsorption capacities for certain metals, the low cost, availability, and minimal pre-treatment requirements of *Prosopis juliflora* make it a competitive alternative to both agricultural waste and algae, especially in low-resource settings. Further studies focusing on real wastewater and field applications would provide a clearer picture of its practical advantages.

Table 5 Adsorption of metal ions using various adsorbents

Type of Biosorbent	Pb ²⁺ (mg/g)	Cd ²⁺ (mg/g)	Cu ²⁺ (mg/g)	References
<i>Prosopis Juliflora</i> Roots	100 - 150	50 - 100	70 - 120	In this study
Rice Husks	30 - 80	20 - 50	50 - 70	Okoro et al., 2022
Banana Peels	60 - 120	40 - 70	50 - 100	Jahin et al., 2024
Algae	150 - 200	120 - 180	100 - 180	Machado et al., 2024
Sugarcane Bagasse	50 - 100	40 - 80	60 - 90	Praipipat et al., 2023

4 Conclusions

The *Prosopis Juliflora* Root Powder (PJRP) possesses pollutant binding properties which can be extremely useful in water treatment. *Prosopis juliflora* roots-based activated carbon can be extremely useful for removing heavy metals from the water. The present research focused on assessing the potential of *Prosopis juliflora* root powder (PJRP) biomass for removing Pb, Cd, and Cu metal ions from water. The investigation revealed that the highest removal efficiencies for these

metals were observed at a pH of 4.0, with Pb achieving a removal efficiency of 94.9290.2%, Cd of 89.7392.2%, and Cu reaching 90.2894.9%. The process of metal ion adsorption using PJRP follows both Langmuir and Freundlich isotherms indicating the multilayer heterogeneous adsorption. The applicability of pseudo-second-order kinetic confirms the rate-controlling process of adsorption. Thermodynamic properties indicated that Gibbs free energy has negative values, indicating a spontaneous process. The results from this study suggest carbonyl, hydroxyl, and alkene functional groups are the main adsorption sites in sugarcane bagasse and the PJRP.

References

- Adeyemi O. Dada, Folahan A. Adekola, Ezekiel O. Odebunmi, Adeniyi S. Ogunlaja and Olugbenga S. Bello (2021). Two–three parameters isotherm modeling, kinetics with statistical validity, desorption and thermodynamic studies of adsorption of Cu (II) ions onto zerovalent iron nanoparticles, *Scientific Reports*, 11, 16454. <https://doi.org/10.1038/s41598-021-95090-8>
- Ahmed Eleryan, Uyiosa O. Aigbe, Kingsley E. Ukhurebor, Robert B. Onyancha, Tarek M. Eldeeb, Mohamed A. El-Nemr, Mohamed A. Hassaan, Safaa Ragab, Otolorin A. Osibote, Heri S. Kusuma, Handoko Darmokoesoemo and Ahmed El Nemr (2022). Copper(II) ion removal by chemically and physically modified sawdust biochar. *Biomass Conversion and Biorefinery*. <https://doi.org/10.1007/s13399-022-02918-y>
- Amit Kumar Dey, Abhijit Dey and Rumi Goswami (2022). Adsorption characteristics of methyl red dye by Na₂CO₃-treated jute fibre using multi-criteria decision-making approach, *Applied Water Science*, 12, 179. <https://doi.org/10.1007/s13201-022-01700-9>
- Candamano S, A. Policicchio, G. Conte, R. Abarca, C. Algieri, S. Chakraborty, S. Curcio, V. Calabrò, F. Crea and R.G. Agostinobc (2022). Preparation of foamed and unfoamed geopolymer/NaX zeolite/activated carbon composites for CO₂ adsorption, *Journal of Cleaner Production*, 330, 129843. <https://doi.org/10.1016/j.jclepro.2021.129843>
- Chuanbin Wang, Xutong Wang, Ning Li, Junyu Tao 2, Beibei Yan, Xiaoqiang Cui and Guanyi Chen (2022). Adsorption of Lead from Aqueous Solution by Biochar: A Review. *Clean Technologies*, 4, 629 – 652. <https://doi.org/10.3390/cleantechno4030039>
- Hana Boubaker, Rim Ben Arfi, Karine Mougin, Cyril Vaultot, Samar Hajj, Philippe Kunneman, Gautier Schrodj and Achraf Ghorbal (2021). New optimization approach for successive cationic and anionic dyes uptake using reed-based beads, *Journal of Cleaner Production*, 307, 127218. <https://doi.org/10.1016/j.jclepro.2021.127218>
- Jahin, H.S., Khedr, A.I. & Ghannam, H.E. Banana peels as a green bioadsorbent for removing metals ions from wastewater. *Discov Water* 4, 36 (2024). <https://doi.org/10.1007/s43832-024-00080-2>

- Jayachandran Sheeja, Krishnan Sampath and Ramasamy Kesavasamy (2021). Experimental Investigations on Adsorption of Reactive Toxic Dyes Using Hedyotis umbellate Activated Carbon, Adsorption Science and Technology, ID – 5035539. <https://doi.org/10.1155/2021/5035539>
- Jinzhen Ma, Liyuan Hou, Ping Li, Shumim Zhang and Xiangyu Zheng (2022). Modified fruit pericarp as an effective biosorbent for removing azo dye from aqueous solution: study of adsorption properties and mechanisms, Environmental Engineering Research, 27 (2), 200634. <https://doi.org/10.4491/eer.2020.634>
- Long Su, Haibo Zhang, Kokyo Oh, Na Liu, Yuan Luo, Hongyan Cheng, Guosheng Zhang and Xiaofang He (2021). Activated biochar derived from spent Auricularia auricula substrate for the efficient adsorption of cationic azo dyes from single and binary adsorptive systems, Water Science & Technology, 84 (1), 101 – 121. <https://doi.org/10.2166/wst.2021.222>
- [Machado, A.A., Valiarampil, J.G. & M, L. Unlocking the Potential of Algae for Heavy Metal Remediation. Water Air Soil Pollut 235, 629 \(2024\). https://doi.org/10.1007/s11270-024-07436-3](https://doi.org/10.1007/s11270-024-07436-3)
- Melánia Feszterová, Lýdia Porubcová and Anna Tirpáková (2021). The Monitoring of Selected Heavy Metals Content and Bioavailability in the Soil-Plant System and Its Impact on Sustainability in Agribusiness Food Chains, Sustainability, 13, 7021. <https://doi.org/10.3390/su13137021>
- Mohammed Benjelloun, Youssef Miyah, Gulsun Akdemir Evrendilek, Farid Zerrouq Sanae Lairini (2021). Recent Advances in Adsorption Kinetic Models: Their Application to Dye Types, Arabian Journal of Chemistry, 14 (4), 103031. <https://doi.org/10.1016/j.arabjc.2021.103031>
- Nadir Khan, Fazal Wahid, Qamar Sultana, Najm Us Saqib and Muhammad Rahim (2020). Surface oxidized and un-oxidized activated carbon derived from Ziziphus jujube Stem, and its application in removal of Cd (II) and Pb (II) from aqueous media. SN Applied Sciences, 2, 753. Doi: <https://doi.org/10.1007/s42452-020-2578-6>
- Nyemaga Malima, Shesan John Owonubi, E. H. Lugwisha and A. S. Mwakaboko (2021). Thermodynamic, isothermal and kinetic studies of heavy metals adsorption by chemically modified Tanzanian Malangali kaolin clay. International Journal of Environmental Science and Technology, 18 (10), 1-16. <http://dx.doi.org/10.1007/s13762-020-03078-0>
- [Okoro, H.K., Alao, S.M., Pandey, S. et al. Recent potential application of rice husk as an eco-friendly adsorbent for removal of heavy metals. Appl Water Sci 12, 259 \(2022\). https://doi.org/10.1007/s13201-022-01778-1](https://doi.org/10.1007/s13201-022-01778-1)

[Praipipat, P., Ngamsurach, P. & Sanghuayprai, A. Modification of sugarcane bagasse with iron\(III\) oxide-hydroxide to improve its adsorption property for removing lead\(II\) ions. *Sci Rep* 13, 1467 \(2023\). <https://doi.org/10.1038/s41598-023-28654-5>](https://doi.org/10.1038/s41598-023-28654-5)

Prasanna Kumar Obulapuram, Tanvir Arfin, Faruq Mohammad, Sachin K. Khiste, Murthy Chavali, Aisha N. Albalawi and Hamad A. Al-Lohedan (2021). Adsorption, Equilibrium Isotherm, and Thermodynamic Studies towards the Removal of Reactive Orange 16 Dye Using Cu(I)-Polyaniline Composite, *Polymers*, 13 (20), 3490. <https://doi.org/10.3390/polym13203490>

Priya A.K, V. Yogeshwaran, Saravanan Rajendran, Tuan K.A. Hoang, Matias Soto-Moscoso, Ayman A. Ghfar and Chinna Bathula (2022). Investigation of mechanism of heavy metals (Cr^{6+} , Pb_{2+} & Zn^{2+}) adsorption from aqueous medium using rice husk ash: Kinetic and thermodynamic approach, *Chemosphere*, 286, 131796. <https://doi.org/10.1016/j.chemosphere.2021.131796>

Ramiro Picoli Nippes, Paula Derksen Macruz, Luiza Carla Augusto Molina and Mara Heloisa Neves Olsen Scaliante (2022). Hydroxychloroquine Adsorption in Aqueous Medium Using Clinoptilolite Zeolite, *Water, Air, & Soil Pollution*, 233, 287. <https://doi.org/10.1007/s11270-022-05787-3>

Rupa Chakraborty, Anupama Asthana, Ajaya Kumar Singh, Bhawana Jain and Abu Bin Hasan Susan (2022). Adsorption of heavy metal ions by various low-cost adsorbents: a review, *International Journal of Environmental Analytical Chemistry*, 102 (2), 342 – 349. <https://doi.org/10.1080/03067319.2020.1722811>

Serdar Aydina, Hamda Mowlid Nura, Abdoulaye Mamadou Traorea, Eren Yıldıırım and Serkan Emik (2021). Fixed bed column adsorption of vanadium from water using amino-functional polymeric adsorbent, *Desalination and Water Treatment*, 209, 280 – 288. [10.5004/dwt.2021.26493](https://doi.org/10.5004/dwt.2021.26493)

Tabrez Alam Khan, Md. Noumana, Divya Dua, Suhail Ayoub Khan and Salman S. Alharthi (2022). Adsorptive scavenging of cationic dyes from aquatic phase by H_3PO_4 activated Indian jujube (*Ziziphus mauritiana*) seeds based activated carbon: Isotherm, kinetics, and thermodynamic study, *Journal of Saudi Chemical Society*, 26 (2), 101417. <https://doi.org/10.1016/j.jscs.2021.101417>

Uduakobong A. Edet and Augustine O. Ifelebuegu (2020). Kinetics, Isotherms, and Thermodynamic Modeling of the Adsorption of Phosphates from Model Wastewater Using Recycled Brick Waste, *Processes*, 8, 665. <https://doi.org/10.3390/pr8060665>

Venkatraman Y and A.K. Priya (2021). Removal of heavy metal ion concentrations from the wastewater using tobacco leaves coated with iron oxide nanoparticles, *International Journal of*

Environmental Science and Technology, 19, 2721–2736. <https://doi.org/10.1007/s13762-021-03202-8>

Yan C.Z, M. G. Kim, H. U. Hwang, A. M. Nzioka, Y. J. Sim and Y. J. Kim (2020). Adsorption of Heavy Metals Using Activated Carbon Synthesized from the Residues of Medicinal Herbs, Theoretical Foundations of Chemical Engineering, 54, 973 – 982. <https://doi.org/10.1134/S0040579520050474>

Yogeshwaran V and A.K. Priya (2021). Experimental studies on the removal of heavy metal ion concentration using sugarcane bagasse in batch adsorption process, Desalination and Water Treatment, 224, 256 – 272. [10.5004/dwt.2021.27160](https://doi.org/10.5004/dwt.2021.27160)

ACCEPTED MANUSCRIPT